
Article:
Acharyya, K, Herbst, E, Caravan, RL et al. (2015) The importance of OH radical–neutral low temperature tunnelling reactions in interstellar clouds using a new model. Molecular Physics, 113 (15-16). 2243 - 2254. ISSN: 0026-8976

https://doi.org/10.1080/00268976.2015.1021729

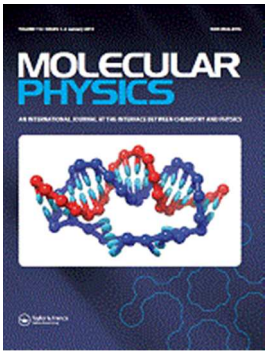

The Importance of OH Radical-Neutral Low Temperature Tunneling Reations in Interstellar Clouds Using a New Model

Journal:	*Molecular Physics*
Manuscript ID:	TMPH-2014-0578.R1
Manuscript Type:	Special Issue Paper
Date Submitted by the Author:	n/a
Complete List of Authors:	Acharyya, Kinsuk; University of Virginia, Chemistry Herbst, Eric; University of Virginia, Chemistry Caravan, Rebecca; University of Leeds, Chemistry Shannon, Robin; University of Leeds, Chemistry Blitz, M.; University of Leeds, Chemistry Heard, D W; University of Leeds, Chemistry
Keywords:	interstellar clouds, gas-grain models

Molecular Physics
Vol. 00, No. 00, Month 2009, 1–18

RESEARCH ARTICLE

The Importance of OH Radical-Neutral Low Temperature Tunneling Reactions in Interstellar Clouds Using a New Model

K. Acharyya[a], E. Herbst[a],* R. L. Caravan[b], R. J. Shannon[b], M. A. Blitz[b] and D. E. Heard[b]

[a] *Department of Chemistry, University of Virginia, McCormick Road, Charlottesville, VA 22904, USA*; [b] *School of Chemistry, University of Leeds, Leeds, LS2 9JT, UK*

(*v4.5 released September 2009*)

Recent laboratory experiments using a pulsed Laval nozzle apparatus have shown that reactions between a neutral molecule and the radical OH can occur efficiently at low temperatures despite activation energy barriers if there is a hydrogen-bonded complex in the entrance channel which allows the system to tunnel efficiently under the barrier. Since OH is a major radical in the interstellar medium, this class of reactions may well be important in the chemistry that occurs in the gas phase of interstellar clouds. Using a new gas-grain chemical network with both gas-phase reactions and reactions on the surfaces of dust particles, we studied the role of OH-neutral reactions in dense interstellar clouds at 10 K, 50 K, and 100 K. We determined that at least one of these reactions can be significant, especially at the lowest temperatures studied, where the rate constants are large. It was found in particular that the reaction between CH_3OH and OH provides an effective and unambiguous gas-phase route to the production of the gaseous methoxy radical (CH_3O), which has been recently detected in cold, dense interstsellar clouds. The role of other reactions in this class is explored.

Keywords: interstellar clouds; gas-grain models

1. Introduction

It is a distinct pleasure to contribute to this special issue of Molecular Physics, entitled "The Molecular Physics of Interstellar Space," in honour of John P. Maier, whose important research in spectroscopy and astrochemistry we are celebrating. This paper discusses some recent improvements to our chemical simulations of interstellar clouds, which can range in size to upwards of 10-100 light years. These clouds are composed of cold gas and sub-micron sized particles, known as dust grains, and can have a rich chemistry. As of the present, around 200 molecules have been detected in interstellar clouds using various spectroscopic techniques, mainly rotational spectroscopy. Although the dominant molecule in the interstellar medium is molecular hydrogen, the majority of the gas-phase molecules are organic in nature with structures that contain up to 13 atoms [1]. Other regions of the spectrum have also been utilised. In the infrared, both non-polar gaseous species (e.g. H_3^+, C_2H_2) and ice mantles, mainly water, surrounding dust particles in cold dense sources have been observed. In addition, the infrared has been used to study both fullerenes (C_{60}, C_{60}^+, and C_{70}) and unknown aromatic material, most

* Corresponding author. Email: eh2ef@virginia.edu

ISSN: 00268976 print/ISSN 13623028 online

DOI: 10.1080/0026897YYxxxxxxxx
http://www.informaworld.com

likely polycyclic aromatic hydrocarbons [2, 3]. In the visible and ultra-violet, background stars have been used as sources to study absorption spectroscopy of atoms and molecules in diffuse clouds, which transmit light in these regions with little extinction. Within most dense clouds, where a typical temperature of 10 - 20 K prevails, small regions are collapsing and eventually warming up to form new generations of stars and planets. The evolutionary trail that leads to stars is a complex one with a number of intermediate sources, all of which have unique inventories of molecules which tell us about their physical conditions and lifetimes [1].

The time-dependent kinetics of individual molecules are coupled together in large models, or simulations, which resemble those used in studies of combustion [4]. Modern astrochemical models used to explain the abundance, or concentration, of these molecules contain both gas-phase and grain-surface chemical processes, contained in kinetic equations for each molecule. The gas-phase and solid-state species are coupled by processes of accretion and desorption. Since the discovery of the first molecules in diffuse clouds – CH [5], CH^+ [6] and CN [7] – in the early 1940's, gas-phase synthetic pathways have been widely used to explain observed abundances of many of these molecules, with the exception of H_2, which is formed by the association of hydrogen atoms on grains [8]. Indeed, astrochemical models that ignore the rest of the grain-mantle chemistry are still in existence. Gas-phase exothermic reactions between ions and neutrals form the bulk of the gas phase chemical networks, especially in cold clouds, where important reactions are assumed not to contain activation energy barriers because of the low temperatures present [1]. The role of neutral-neutral reactions has been increasing, as shall be discussed below.

The main starting point for gas-phase interstellar chemistry is the ionization of H_2 by cosmic rays (CR), which are high-energy nuclei, mainly protons, that can penetrate even dense clouds, unlike visible and ultraviolet photons [9]. Following the production of H_2^+, reaction with H_2 leads to H_3^+, which is the precursor for many additional ions; i.e.,

$$H_2 + CR \rightarrow H_2^+ + e^- \quad (1)$$

$$H_2^+ + H_2 \rightarrow H_3^+ + H \quad (2)$$

$$H_3^+ + X \rightarrow H_2 + HX^+, \quad (3)$$

where X represents neutrals with higher proton affinities than molecular hydrogen. In dense clouds, where H_2 is overwhelmingly greater in concentration than any other species, the H_2^+ ion, which reacts rapidly with H_2, is short lived ($\sim$ few hours) compared with other astrophysical time scales. As a result, reactions with H_3^+ and neutral atoms, mainly O and C, provide the gateway for the formation of other ionic species. For example, the reaction between H_3^+ and O produces the ion OH^+, which, via H-atom transfer reactions with H_2, leads to the short-lived ion H_2O^+ and eventually to the longer-lived ion H_3O^+. The production of the neutral species OH and H_2O then occurs via dissociative recombination reactions between this ion and electrons [10].

The dominance of ion-neutral reactions in astrochemical models of cold regions started in the first serious models in the 1970's because it was thought that most neutral-neutral exothermic reactions have barriers, which make them inefficient at the prevailing low temperatures. Small numbers of radical-radical reactions, known to be barrierless (at least at the higher temperatures studied in the laboratory) were included [11]. The first major extension of the models of cold sources to include other classes of neutral-neutral reactions began as a result of studies using a con-

tinuous flow technique with Laval nozzles known as CRESU (a French acronym for Cinétique de Réaction en Encoulement Supersonique Uniforme) [12]. The CRESU technique can measure reaction rate constants down to ≈ 10 K and even below [13]. Eventually a significant number of barrierless reactions of the radical-neutral category were measured down to low temperatures from 300 K and found to have large rate constants with either no temperature dependence or with a small inverse temperature dependence [14]. At low temperatures, these reaction rate constants can approach the results of simple collision theories. It was then found that for some important interstellar molecules, radical-neutral pathways could compete with ion-molecule/dissociative recombination pathways. Based on a survey of the results for reactions between radicals and alkenes and alkynes, two criteria have been proposed in order to predict if reactions of this type will have rate constants greater than $\sim 10^{-10}$ cm^3 s^{-1} at 10 K [15]. The first criterion is that the rate constant at 298 K should be greater than $\sim 10^{-11}$ cm^3 s^{-1}; the second criterion is that the difference between the ionization energy of the neutral molecule and the electron affinity of the radical must be greater than 8.75 eV.

As temperature increases significantly above the ambient value in cold clouds, neutral-neutral reactions with small activation energies and/or endothermicities can become important. Neutral-neutral reactions in the temperature range of ∼200-400 K are widely studied in the context of the terrestrial atmosphere. These are regularly being updated in two websites (http://www.iupac-kinetic.ch.cam.ac.uk and http://jpldataeval.jpl.nasa.gov). Analogous reactions, but involving interstellar molecules, could be used for warmer regions of interstellar clouds such as hot cores, where the formation of a protostar heats up surrounding collapsing material to 100-300 K. Reactions at even higher temperature can become important at subsequent stages of star formation regions, such as protoplanetary disks, the direct precursors to star and planets. Kinetic data for such reactions can be found in studies of combustion chemistry [16].

Most recently, it has even been found that certain radical-neutral reactions with activation energy barriers can be rapid at low interstellar temperatures. With the pulsed Laval nozzle technique, the Leeds group [17–19] have uncovered a new type of mechanism for OH-neutral systems in which the reaction rate constant for systems with activation energy barriers can increase significantly at low temperatures as the temperature decreases. The mechanism that causes this effect requires a potential well in the entrance channel as well as tunneling through the barrier. The potential well corresponds to a hydrogen-bonded complex, which becomes sufficiently long-lived at low temperatures to increase the efficiency of tunneling under the later barrier. In their first measurement, it was found that the rate coefficient for the reaction between the OH radical and CH_3OH increases by more than two orders of magnitude when the temperature is reduced from ∼ 200 K to 56 K [17, 20]. Later measurements showed similar effects for reactions between OH and organic species such as acetone, dimethyl ether, and ethanol [18, 19]. Using the MESMER (Master Equation Solver for Multi Energy Well Reactions) code to fit their experimental data, Shannon et al. [18] were also able to obtain the rate coefficients down to lower temperatures. For the OH + CH_3OH reaction, this modelling was accomplished down to 10 K. For the other systems, a simple extrapolation of the data down to temperatures as low as 20 K can also be attempted, but with uncertainty. By this temperature, the extrapolated value of the rate constant can be as high as 3×10^{-10} cm^{3}s^{-1}, suggesting that at temperatures relevant to cold cores, almost every collision between, for example, OH and CH_3OH results in reaction, in this case leading to methoxy (CH_3O), a known interstellar molecule [21]. A complete list of the published reactions can be found in Table 1. **The actual rate**

constants used in our calculations will be discussed later in the text. It was also concluded that this phenomenon could be widespread under the low temperature conditions found in interstellar space.

The goals of this paper are to present our new gas-grain chemical network, and, using this network, to report a study of the impact of fast neutral-OH radical reactions in the astrochemical modeling of cold regions. In the next section, we discuss our reaction network, then in Section 3, the determination of selected classes of rate constants is discussed. In Section 4, the results of our simulation are presented, while in Section 5, we present our conclusions.

Table 1. Studied OH-Neutral Reactions

No.	Reactions	Reference
1.	$OH + CH_3OH \rightarrow CH_3O + H_2O$	Shannon et al.[17] Gomez-Martin et al.[20]
2.	$OH + CH_3COCH_3 \rightarrow CH_3COCH_2 + H_2O$	Shannon et al.[18]
3.	$OH + CH_3OCH_3 \rightarrow CH_3OCH_2 + H_2O$	Shannon et al.[18]
4.	$OH + CH_3CH_2OH \rightarrow CH_3CH_2O + H_2O$	Caravan et al.[19]
5.	$OH + CH_3CHOHCH_3 \rightarrow CH_3CHOCH_3 + H_2O$	Caravan et al.[19]

2. Chemical Network

2.1. *Gas Phase Chemical Networks*

To study the molecular complexity observed in the variety of astrophysical sources, one needs chemical networks that contain reaction rate constants. Until recently, there were two main chemical databases of gas phase chemistry to study chemical evolution in the interstellar medium. The first one is the UDfA database, previously labelled the UMIST database (http://www.udfa.net/) and the second one is the OSU database (http:/faculty.virginia.edu/ericherb). The OSU database is perhaps more relevant for cold sources ($\sim$ 10 K), whereas the UDfA database includes many reactions for warmer regions ($>$ 100 K) of the interstellar medium. Both of these databases are primarily local products, maintained by the faculty and students at the University of Manchester Institute of **Science and** Technology (now primarily Queens University Belfast) and Ohio State University (now the University of Virginia), respectively. Entries into the databases are obtained from experiments, theory, and estimates. Recently, another network was created primarily based on the OSU network. Known as the KIDA database (http://kida.obs.u-bordeaux1.fr), an acronym for Kinetic Database for Astrochemistry, this database includes gas-phase chemical reactions suitable for both astronomical environments and planetary atmospheres that are grouped into either networks supplied by the database organisers or that can be attuned to individual tastes. KIDA is maintained at the University of Bordeaux, but is supervised by a group of international experts in the various types of reactions. One major advantage of the KIDA network is that along with the chemical reactions, it also provides the temperature range for which each reaction rate constant is measured, calculated, or estimated. Both the UDfA and KIDA networks come along with algorithms for calculating molecular concentrations as a function of time, depending upon fixed physical conditions. Algorithms for more complex physical conditions – both heterogeneous and/or time-dependent – also exist. One prime example is the Meudon PDR network and code

(http://pdr.obspm.fr/PDRcode.html) which is designed for photon-dominated regions, defined as regions near stars, in which the chemistry is a strong function of the distance from the star.

Another important class of gas-phase reactions that is missing in the KIDA network consists of gas-phase reactions for forming complex molecules in hot cores, which contain warming material between 100 K and 300 K. However, these reactions are included in a variant of the OSU database that is designed for complex molecule formation at these temperatures [22]. We label this network Garrod08. This network is mainly associated with the formation of complex molecules on grain surfaces, which is discussed below. The ion-neutral gas-phase reactions in Garrod08 produce larger ions. An example is the radiative association reaction

$$CH_3^+ + HCOOH \rightarrow HC(OH)OCH_3^+ + h\nu, \quad (4)$$

where the product ion can subsequently undergo dissociative recombination with electrons to produce methyl formate, a common interstellar molecule in hot cores.

To include all these aspects, we constructed a new gas-phase network by adding the following three components:

- reactions between 10 K and 800 K from the kida.uva.2011 network with some additions/revisions,
- reactions for the formation and destruction of complex molecules from the Garrod2008 network but not in the KIDA database; rate constants extended to 800 K,
- OH-neutral reactions listed in Table 1 except for the one involving $CH_3CHOHCH_3$. At present, these rate constants are used in the range 10 K - 100 K only.

Although we initially utilised a KIDA network that was assembled in 2011 [4], we subsequently added reactions/rate constants that had been added or revised afterwards; these will soon be included in a new KIDA network (kida.uva.2014).

Rate constants in the KIDA database come with four possible recommendations for users:

- Not recommended. This recommendation suggests strongly that the reaction not be included in individual networks.
- Unknown. These reactions have not been looked at by an expert.
- Valid. These reactions are associated with a bibliographic reference.
- Recommended. These reaction rate constants can be used with the assigned uncertainties.

Rate constants that come with either a valid or recommended tag are included in our network. Selected rate constants that come with an unknown tag have been considered by us and assigned a rate constant normally by analogy with other studied systems. The gas-phase network contains in total approximately 8670 reactions involving 670 gas-phase species.

In compiling the gas-phase reaction network from different sources, we used previous measurements, calculations, or estimates of rate constants down to a lower limit of 10 K. We considered 800 K as a feasible upper temperature limit based on existing data and the need for a high limit considering evidence of chemistry at such high temperatures in various interstellar regions [23]. The temperature dependence for assorted reaction types will be considered later in the paper. For those reactions for which the rate coefficient is not available up to 800 K, either we simply enlarged the temperature range upwards or modified the rate coefficient such that it is likely to be valid up to 800 K.

2.2. *Gas-Grain Chemical Network*

There is no open database that provides grain surface reactions and their rate constants, although networks including grain-surface reactions can be obtained from several sources such as the Virginia group (http: faculty.virginia.edu/ericherb). The surface reactions are assumed to occur via diffusion on grain surfaces, a process known as the Langmuir-Hinshelwood mechanism, and sticking of gas-phase reactants to grain surfaces occurs via physisorption. At low temperatures, the only species that can diffuse readily are atoms and diatomic molecules, whereas as the temperature increases from 10 K to temperatures higher than 100 K, as in hot cores, larger species can diffuse and take part in reactions, mainly leading to association. The surface reactions in Garrod08 contain both of these types of processes, and form the basis for the surface reactions in our network. The reactions occurring in cold regions eventually build up ice mantles on grains, with water the dominant species and CO, CO_2 and CH_3OH among the more abundant species as well. Surface reactions involving molecules normally contain activation energy barriers unless the species are activated by granular bombardment by charged particles and photons, which convert them into radicals. In our network, photon bombardment is assumed with the fragments governed by gas-phase cross sections for photodissociation, a strong approximation. Following radical-radical association into still larger species, the products eventually desorb into the gas phase, where they can be more easily detected. As an example, consider methanol and fomaldehyde on a grain surface. Photodissociation can produce the methoxy radical from methanol and the formyl radical (HCO) from formaldehyde. Association of the two radicals can lead to methyl formate ($HCOOCH_3$), although this reaction has yet to be studied in the laboratory.

The rates of reaction for binary surface reactions are normally treated by rate constants in which diffusion is modeled by series of individual hopping or tunneling motions from one surface binding site to a nearest neighbor [24]. More exact treatments use stochastic approaches, since in many instances there are few reactive species on each grain and fluctuations are critical [25]. For example, there is often an average value of H atoms on grains which is less than unity, yet it takes two H atoms on an individual grain to produce the H_2 molecules detected in the gas [8].

For the grain surface reactions, we considered the dust temperature range to be 10 K to 800 K, as in our gas phase network. The two temperatures need not be the same. In addition, it is to be noted that reactions at temperatures above 200 K on the grain surface are not important since grains cannot retain molecules above 200 K, unless chemisorption sites are used [8, 26, 27]. We have not added any chemisorption reactions in this network. On the grain surface we have considered 2764 reactions among 247 grain surface species. New reactions are being studied at a rapid rate thanks to a number of groups in places such as Leiden, Syracuse, NY, Sapporo, and Paris that specialise in low temperature surface and ice chemistry. The assorted abundances of species in the gas and granular phases are coupled via accretion and desorption processes. These processes are discussed in detail in the next section.

3. Rate Constants Utilised

3.1. *Gas phase reactions*

Based principally on tabulated rate constants from measurements appearing in the NIST Chemical Kinetics Database (kinetics.nist.gov/kinetics/index.jspwe) for neutral-neutral processes, we store the rate constants of bimolecular processes in

the form of a modified Arrhenius formula:

$$k_{ij}(T) = \alpha(T/300)^{\beta} \exp(-\gamma/T) \text{ cm}^3\text{s}^{-1} \quad (5)$$

where α, β and γ are parameters.[1] For some reactions, different values of the parameters are needed for different temperature ranges. Rate constants for radical-neutral reactions typically are based on experimental results. Suitable low temperature results for cold interstellar clouds come from measurements or extrapolations of CRESU and pulsed-nozzle Laval techniques [14, 15, 18], as discussed above. Anicich has compiled a long list of relevant rate constants for ion-neutral reactions [28].

For ion-neutral reactions not studied in the laboratory, specific rate expressions are used depending upon whether or not the neutral reactant is polar or non-polar. For non-polar reactants, the temperature-independent Langevin value:

$$k_{\text{L}} = 2\pi e(\alpha/\mu)^{1/2} \quad (6)$$

is used, where α is the dipole polarizability and μ is the reduced mass of the reactants. The Langevin rate constant, which is based on a long-range central-force capture approximation, has a value of $\approx 10^{-9}$ cm^3 s^{-1}, which is 1-2 orders of magnitude greater than the gas kinetic value. It is known to be an excellent approximation. Of course, the expression for k_{L} does not yield the products, which must be barrierless. The products of reactions can normally be obtained by a mixture of thermodynamics and measurements on analogous sytems. Rate constants k_{D} for reactions between ions and neutral species with a dipole moment are computed using the more complex Su-Chesnavich capture approach since the system is no longer a central force one [29]. The rate constant k_{D} is expressed in terms of k_{L} using two formulae, one for a lower temperature range and the other for a higher temperature range. The unitless parameter x used to divide the temperature range is defined by the equation

$$x = \frac{\mu_{\text{D}}}{(2\alpha kT)^{1/2}} \quad (7)$$

where μ_{D} is the dipole moment. When x is ≥ 2, the formula for $k_{\text{D}}/k_{\text{L}}$ is given by

$$k_{\text{D}}/k_{\text{L}} = 0.4767x + 0.6200, \quad (8)$$

while when x is < 2, the formula becomes

$$k_{\text{D}}/k_{\text{L}} = (x + 0.5090)^2/10.526 + 0.9754. \quad (9)$$

At the lowest temperatures, k_D goes as $T^{-1/2}$, whereas at the highest temperatures, it approaches the Langevin value.

Another important class of binary reactions to be discussed here consists of dissociative recombination reactions between positive molecular ions and electrons, which have been studied mainly in storage rings [10]. The total rate coefficients for these reactions are typically 10^{-7} - 10^{-6} cm^3 s^{-1} at 300 K with a temperature dependence of $T^{-1/2}$. There are typically a number of exothermic neutral channels, the relative weights of which must be determined experimentally.

[1]It is customary in chemical kinetics involving ions to use the cgs-esu unit system, which is also the dominant system in astronomy. For these reasons, SI units have not been utilised.

In addition to the classes of bimolecular reactions discussed above, processes in which a complex is formed and stabilised by the emission of a photon are critical in the cold interstellar medium. Two processes exist: (1) radiative association, in which two gas-phase molecules collide to eventually form a larger product, and (2) radiative attachment, in which a stable negative ion is formed by collision of a neutral molecule and an electron. Statistical theories have been formulated for both processes, since few experiments have been done [30, 31].

Unimolecular rate constants are used for photo-processes involving UV photons. The first-order rate constants for these processes are parameterised as a function of the dust visual extinction A_V, which is an astronomical parameter similar to the optical depth τ; the term 'visual' refers to a range of wavelengths used in classical photographic plates. For a diffuse cloud, $A_V \approx$ 1-2, while for a dense cloud $A_V \geq 10$. The rate constant can then be approximated by the expression

$$k_{\rm photo} = \alpha \exp(-\gamma A_V) \ {\rm s}^{-1}. \tag{10}$$

The parameter α represents the photodissociation rate in an unshielded average interstellar radiation field and the parameter γ takes into account the fact that photodissociation takes place in the UV; typically $\gamma \approx$ 2-3 since the extinction due to dust is greater in the UV than in the visual.

Another unimolecular rate constant is needed to describe the rate of ionization as caused by cosmic rays. This rate constant is given by the expression

$$k_{\rm CR} = \alpha\zeta \ {\rm s}^{-1} \tag{11}$$

where $\alpha = 1$ for atomic hydrogen and has a different value for each atom or molecule. The ionization rate constant for hydrogen atoms, ζ (s^{-1}), ranges from 10^{-15} s^{-1} in the more diffuse clouds to 10^{-17} s^{-1} in dense clouds, depending upon the degree of penetration [32]. Cosmic rays can also produce internal UV photons by excitation of molecular hydrogen; these photons play an important role in dense clouds where external UV and visible photons cannot penetrate due to the high visual extinction [33]. Rate constants for other processes can be found in review articles [34].

In total, eight major classes of gas phase reactions are used in our network, as described in Table 2, which is essentially the KIDA division of classes [4]. (See also http://kida.obs.u-bordeaux1.fr.)

3.2. *Grain surface/mantle reactions*

Before any diffusive grain reaction can occur, a gas-phase species must be adsorbed onto a grain. The rate of adsorption, $r_{ad}(j)$ (s^{-1}), for a given gaseous species j onto a single grain is expressed as

$$r_{\rm ad}(j) = S_j \sigma v_j n_j \tag{12}$$

where S_j is the probability of sticking to the grain, σ is the granular cross section (cm^2), v_j is the velocity **of the j-th adsorbing gas-phase species and n_j (cm^{-3}) is its number density.** We normally assume that the probability of sticking is unity or 0.5.

Adsorbed species react by encountering other species as they diffuse around the grain surface. The rate of diffusion for an individual species on a single grain is related to the rate of thermal hopping (s^{-1}) from one binding site to a nearest

Table 2. Reaction Classes for Gas-Phase Reactants

Type	Name of the Reaction	Description
1.	Direct CR processes	Dissociation/ionization of species due to collision with cosmic rays
2.	CR induced photo processes	Dissociation/ionization of species due to secondary UV photons
3.	Photo processes	Dissociation/ionization of species due to external interstellar UV field
4.	Bi-molecular reactions	Includes neutral-neutral, ion-neutral, anion-cation and associative ionization reactions
5	Charge Exchange reactions	Reaction between two oppositely charged particles
6.	Radiative Association	Association reaction between two species stabilised by the emission of a photon
7.	Associative detachment	Association of a neutral species and an anion resulting in the ejection of the extra electron
8.	Dissociative recombination and radiative attachment	Recombination of a positive ion with an electron resulting in the dissociation of the parent neutral or the emission of a photon following the attachment of an electron to a neutral radical

neighbour site, which is given by the expression [24]

$$r_{\rm hop} = \nu_0 \exp(-E_{\rm b}/T_{\rm d}). \quad (13)$$

Here $E_{\rm b}$ is the energy barrier (K) between binding sites, which is a function of both the adsorbate and the surface, $T_{\rm d}$ is the grain temperature, and ν_0 is the characteristic vibrational frequency, or 'attempt frequency', which is measured or estimated to be 1-3 $\times 10^{12}$ s^{-1} for physisorbed species. The energy barrier is often estimated as a fraction (0.3 - 0.8) of the binding energy of the adsorbate, $E_{\rm D}$ (K). The diffusion rate for a given adsorbate, $r_{\rm diff}$, which is the hopping rate over the total number of binding sites $N_{\rm s}$ on the surface of a grain, is given by

$$r_{\rm diff} = r_{hop}/N_{\rm s}. \quad (14)$$

The surface reaction rate constant between two individual species i and j per individual grain is obtained by determining the rate at which two species can occupy the same binding site, which leads to the equation

$$k_{\rm ij} = \kappa_{ij}(r_{\rm diff,i} + r_{\rm diff,j}), \quad (15)$$

where κ_{ij} is the probability for the reaction to occur upon an encounter in a common binding site. The overall rate law per volume for reaction is obtained by multiplying $k_{\rm ij}$ by the number of species of types i and j per grain, and the number of grains per unit volume. The value of κ_{ij} is unity for reactions with no activation energy barrier, while for reactions with an activation energy barrier it can be approximated by the quantum mechanical tunneling probability or the hopping probability, whichever is greater [24, 35]. Quantum mechanical tunneling under diffusion barriers can also add mobility to the diffusing reactive species. We have considered only thermal hopping, however, because **most** recent experiments do not indicate the existence of quantum mechanical tunneling for diffusive motion

[36–38]. **Minissale et al. [39], on the other hand, have interpreted the rapid diffusion of oxygen on olivine at low temperatures as due to tunneling.**

In addition to the diffusive, or Langmuir-Hinshelwood, mechanism, surface reactions can occur via the Eley-Rideal mechanism, in which a gas-phase species collides with an adsorbate, leading to reaction. Although very few reactions that occur via the Eley-Rideal mechanism have been studied in the laboratory, astrochemists have suggested such processes when other mechanisms appear to fail. An example is the explanation of the formation of certain complex molecules in cold regions of the interstellar medium [40]. The network used in the simulations reported here does not contain the Eley-Rideal mechanism.

3.3. *Desorption Processes*

Molecules from the surface will desorb into the gas phase either via thermal desorption, often mistakenly termed evaporation, or via non-thermal mechanisms. The desorption rate ($r_{\rm evap}$) per species is given by an equation similar to the hopping rate but involving the binding energy of the adsorbate:

$$r_{\rm evap} = \nu_0 \exp(-E_{\rm D}/T_{\rm d}); \tag{16}$$

this rate is not effective in cold cores, which are typically at 10 K, except for the lightly bound H and He atoms, and molecular hydrogen. There are several mechanisms for non-thermal desorption included in our model. The first is reactive desorption; here the exothermicity of reaction is channeled into the desorption of the product with an estimated efficiency determined by a parameter $a_{\rm RRK}$ [41]. In the results presented later in the text, we have used a value of 0.01, which roughly translates into an efficiency of 1%. Recent experiments indicate that reactive desorption can be more efficient than this from bare grain surfaces, but not from ice mantles [42]. Secondly, there is desorption by photodissociation. In one process involving photodissociation, two radicals are formed, and can subsequently recombine and then desorb via the reactive desorption mechanism. As is the case for gas-phase species discussed above, the externally generated UV and visible photons are very effective in diffuse clouds but their role in dense clouds is very limited [43]. The rate constants for photodissociation on surfaces are assumed to be the same as in the gas phase. **Recent work shows, however, that this assumption need not be accurate for all species [44–46].**

We have added direct photodesorption by external UV photons and by cosmic ray generated UV photons to this network following recent laboratory measurements [47–49], which show that photodesorption with efficiencies near 10^{-3} per UV photon can occur by a variety of mechanisms when UV photons strike ices of assorted species. **While measured photodesorption yields for CO, N_2, CO_2 H_2O and CH_3OH have been utilised in our network, we also assume that a similar efficiency occurs for all other species on grain mantles. This assumption is indeed a simplification because the efficiency of photodesorption is still unsettled [50, 51]**. Consider a species i that covers N_i sites of a bare grain with $N_{\rm S}$ sites. Then the rate of photodesorption per grain is given by the expression

$$r_{\rm CR,pd} = I_0 A Y_{\rm pd} \frac{N_i}{N_{\rm S}} \tag{17}$$

where $Y_{\rm pd}$ is the photodesorption yield, A is the cross sectional area of the grain,

and I_0 is the UV photon intensity in units of s^{-1} cm^{-2}. Based on experiments, the non-zero yield pertains only to the top several monolayers, even though photon penetration can be much deeper. Now let us make the situation more complex by considering an ice mantle of N_L filled monolayers and a number of species, each of which occupies a given fraction of sites in each monolayer. Then the photodesorption rate of any species j is given by the equation

$$r_{j,\mathrm{CR,pd}} = I_0 A Y_{\mathrm{pd}} N_{\mathrm{L}} \frac{N_j}{N_{\mathrm{S}}} \tag{18}$$

where the number of sites N_S in each filled monolayer is equal to the sum of the numbers of the different species N_1, N_2, ... in that monolayer and the uppermost partially filled monolayer is ignored. One can also use assorted concentration units such as areal concentration to replace the numbers used for each species and the total sites. To derive an overall volume rate, one must multiply by the grain concentration. If we are dealing with cosmic ray photons, the intensity to use for I_0 is a constant 10^4 cm^{-2} s^{-1} whereas for the case of external radiation, we can use the expression

$$I_0 = G_0 \exp(-\gamma A_v), \tag{19}$$

where $G_0(10^8$ photons cm^{-2} $s^{-1})$ is the unattenuated UV photon flux, and γ is a measure of the UV extinction.

Finally, non-thermal desorption can occur via the heating of grains caused by cosmic ray bombardment [52], the rate of which per species is given by

$$r_{\mathrm{CR,d}} = D\nu_0 \exp(-E_{\mathrm{D}}/T_e), \tag{20}$$

where D is the duty cycle of the grains at elevated temperature, and T_e is the elevated temperature due to cosmic ray heating. We have used the values of D (3.19×10^{-19}) and T_e (70 K) from Hasegawa and Herbst [52].

4. Results

Models have been run for homogeneous dense clouds at gaseous **and dust** temperatures of 10 K, 50 K, and 100 K. The rate coefficients for the OH-neutral reactions in Table 1 with the exception of $CH_3CHOHCH_3$ are listed for these three temperatures in Table 3. Some of these results, obtained partially by extrapolation of the measurements of the Leeds group, are reported for the first time. Since the actual measurements go down to only 50 K, the MESMER modelling/extrapolation to the lowest temperature is somewhat uncertain except for the methanol reaction. Based on this result, the values for the rate constants of the reactions at 10 K involving methanol and acetone are probably the most likely values while those involving dimethyl ether and ethanol are probably lower limits. It is exceedingly likely, however, that increasing these lower rate coefficients to those for methanol would not have much effect in the astronomical calculations. Gas-phase initial abundances correspond to the so-called 'low metal' elemental abundances, and are atomic in nature except for molecular hydrogen [53].

The physical parameters of the cloud remain constant throughout the chemical evolution with a standard total hydrogen density $n_H = 2 \times 10^4$ cm^{-3}, where n_H refers to the sum of the concentrations of atomic hydrogen and twice that of molecular hydrogen. In this case, there is very little atomic hydrogen. Other parameters

include a visual extinction $A_V = 10$, a cosmic ray ionization rate $\zeta_{H_2} = 1.3 \times 10^{-17}$ s^{-1}, and a sticking coefficient $S = 0.5$. The grains are assumed to have a standard radius of 0.1 μm and to possess 0.01 of the cloud mass. To calculate desorption and surface reaction rate constants, we used binding energies, E_D, and barriers for hopping, E_b, representative of an amorphous water ice surface [22]. These values are higher than the bare grain values used in earlier models [24]. We used a surface site density $n_s = 1.5 \times 10^{15}$ cm^{-2} [24].

We initially ran three models including only the reaction between OH and CH_3OH, then followed with another three models in which the three additional reactions in Table 3 were included. These reactions were omitted in our first calculations to isolate the effect of the OH + CH_3OH reaction. The reaction between OH and $CH_3CHOHCH_3$ was omitted because this neutral molecule is currently not included in our network.

Figure 1 shows the time variation of the fractional abundances of OH and methanol at 10 K, 50 K, and 100 K with the OH + CH_3OH reaction either on or off. It can be seen that OH is much more abundant than methanol and that whether or not the reaction between the two is on or off has little effect on the abundance of OH. The diminution of methanol when the reaction is turned on is visible, but only at 10 K, where methanol is itself most abundant. Its fractional abundance ranges from 10^{-10} to 10^{-9}, in reasonable agreement with the observed value in the cold core TMC-1. Gas-phase methanol is formed from the surface hydrogenation of CO via successive reactions with atomic hydrogen, followed by non-thermal desorption. The major loss mechanisms for gaseous methanol include reactions with a number of atomic and molecular ions, as well as neutral-neutral reactions with F and Cl atoms leading to the radical CH_2OH. The reactions with F and Cl are not contained in our network. Reaction with OH is generally not an effective destruction route for CH_3OH except for a small time window when methoxy is near its peak.

Table 3. OH-Neutral Rate Constants Used in Models (units: 10^{-10} cm^3 s^{-1})

Reactant	10 K	50 K	100 K
CH_3OH	3.0	0.49	0.38
CH_3COCH_3	1.0	1.0	0.37
CH_3OCH_3	0.30	0.17	0.077
CH_3CH_2OH	0.60	0.60	0.50

Figure 2 shows the time variation of the fractional abundance with respect to hydrogen of methoxy (CH_3O), which is the radical product of the reaction between OH and methanol. The models were also run with and without the OH + CH_3OH reaction. It can be seen that around $t = 2 \times 10^5$ years, models at 10 K and 50 K that include the OH + CH_3OH reaction (solid lines) start to show an increased abundance for CH_3O. The effect is much larger at 10 K because the reaction occurs more rapidly at this temperature. **Note that the increase in methoxy corresponds to a decrease in methanol. Moreover the abundances of methanol and methoxy are very similar although methoxy is more abundant. The abundances are coupled in the sense that methanol is a precursor of methoxy through the reaction with OH, while methoxy is a precursor of methanol through a hydrogenation reaction with atomic hydrogen**

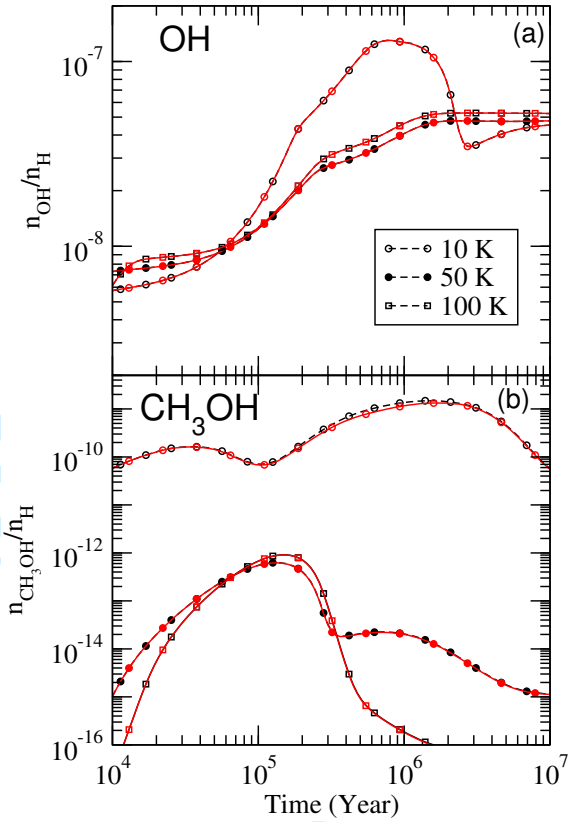

Figure 1. Time evolution of OH and CH_3OH at 10 K, 50 K and 100 K. Solid lines are used to represent abundances when the OH + CH_3OH reaction is included.

on the grain surface. By $t \approx 1 \times 10^6$ years, the abundance of methoxy at 10 K becomes twice as large as the calculated abundance without the reaction. To look more closely at the magnitude of the effect at 50 K and 100 K, we plot the percentage gain in abundance for CH_3O when OH + CH_3OH is included in Figure 3, top panel. At 50 K, the maximum enhancement is 50 %, which occurs at $t \approx 2 \times 10^6$ years while at 100 K the maximum enhancement is a very small 2 %. Figure 3, bottom panel, shows the percentage loss of the CH_3OH abundance due to the OH + CH_3OH reaction. The maximum loss, around 20 %, is seen at 10 K and $t \approx 5 \times 10^5$ years. Like the increase in the CH_3O abundance, this loss decreases as temperature is increased.

The main competitive formation reaction in our model to OH + CH_3OH occurs on grain surfaces:

$$s - H + s - H_2CO \rightarrow s - CH_3O, \qquad (21)$$

which neglects the possibility that the isomer H_2COH is formed. Since experiments indicate a conversion of surface methoxy to H_2COH, it is likely that this competitive mechanism is slower than estimated in our network although detailed calculations are needed for interstellar conditions and time scales. **If the surface mechanism is indeed slower than calculated**, the OH + CH_3OH reaction becomes relatively more important in the formation of methoxy [21]. Grain formation at 10 K requires non-thermal desorption of the products, most likely by photodesorption or reactive desorption. Other gas-phase channels include the dissociative recombination of protonated methanol and electrons and the photodissociation of methanol; all of

the gas-phase channels require the prior formation of methanol on grain surfaces followed by non-thermal desorption into the gas. The OH + CH_3OH reaction has also been included by Balucani et al.[54] in a model of complex molecule formation in cold cores. These authors found the OH + CH_3OH reaction to be the dominant mechanism of methoxy formation. In a previous model of complex molecule formation in cold cores, Vasyunin and Herbst [55] included the channel but did not find it to be competitive given their assumption of rapid reactive desorption **and their use of a smaller rate constant for OH + CH_3OH.**

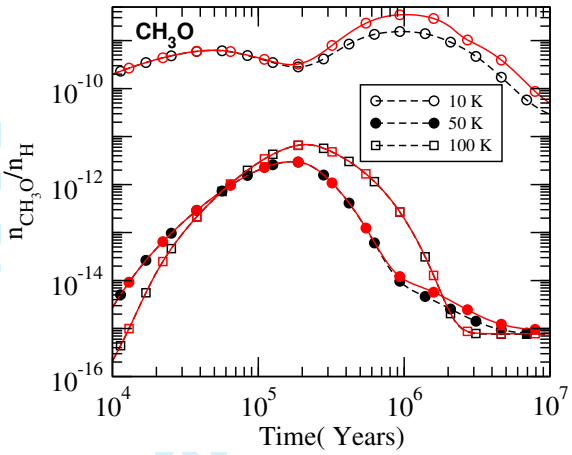

Figure 2. Time evolution of the fractional bundance of CH_3O at 10 K, 50 K and 100 K. Solid lines are used to represent abundances when the OH + CH_3OH reaction is included.

CH_3O has recently been detected towards the cold dense core B1-b using the IRAM 30 metre telescope, and found to have a fractional abundance of $\approx 10^{-11}$ relative to the total hydrogen density [21]. As can be seen in Figure 2, our current model overestimates the methoxy abundance at 10 K. The best overall agreement with observation in cold cores occurs at a time of 10^5 yr; our calculated methoxy abundance at this time is high by a factor of 30. The result of Vasyunin & Herbst [55] is high by a factor of 10; both treatments probably underestimate the destruction rate of methoxy. The models of Balucani et al. [54] can be made consistent with the observed fractional abundance of methoxy at a time of 10^5 yr by increasing the total hydrogen density to 3×10^5 cm^{-3} and the temperature to 20 K.

We now consider models in which all four OH reactions in Table 3 are included. Figure 4 (left panel) shows the time evolution at 10 K of the fractional abundances of acetone (CH_3COCH_3), dimethyl ether (CH_3OCH_3) and ethanol (CH_3CH_2OH), all of which react with OH to produce the acetonyl radical (CH_3COCH_2), the methoxymethyl radical (CH_3OCH_2) and the ethoxy radical (CH_3CH_2O) respectively. It can be seen from Figure 4 that the OH reactions have a small effect; only a minor change is seen for CH_3OCH_3 between $t = 3 \times 10^5$ and $t = 2 \times 10^6$ years.

The product radicals (CH_3COCH_2, CH_3OCH_2 and CH_3CH_2O) shown in Figure 4 (right panel) have been added to our network for completeness. We have not added any destruction pathways for these species, so that the fractional abundances shown should be taken as upper limits. Even in the absence of destruction pathways, the abundances of these molecules are lower than the modern day detection limit, therefore, they may not be observable with the possible exception of the ethoxy radical.

Acetone, dimethyl ether and ethanol, all referred to as complex organic molecules (COMs), have been observed with large fractional abundances ($\approx 10^{-8}$) towards

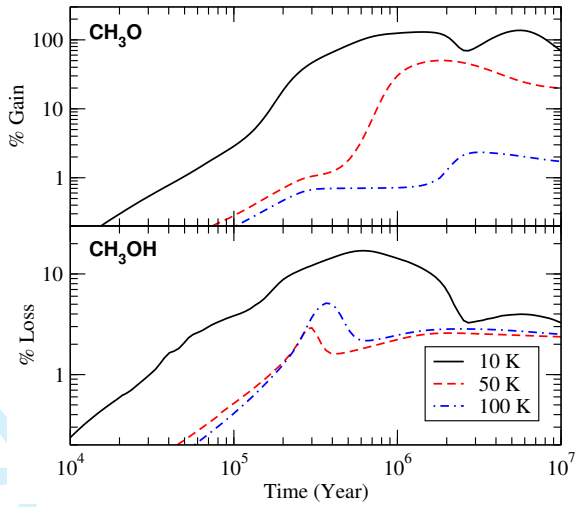

Figure 3. Time variation of % gain/loss in abundance of CH_3O and CH_3OH at 10 K, 50 K and 100 K with the inclusion of the OH + CH_3OH reaction. Lines that are not visible indicate a change of less than 1 %.

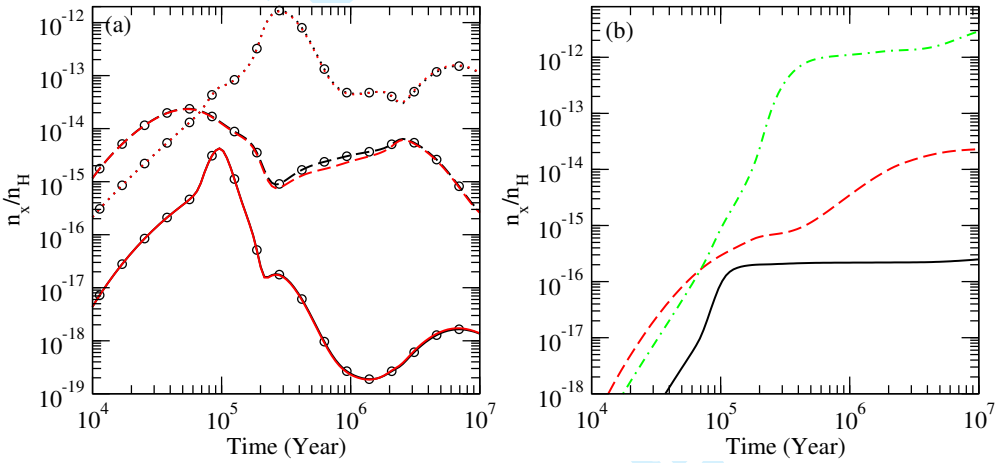

Figure 4. Time evolution of the fractional abundances of assorted reactants (left panel) and radical products (right panel) of OH reactions at 10 K. Left panel: Solid line represents acetone, dashed line represents dimethyl ether, and dotted line represents ethanol. The line without circles for dimethyl ether represents the situation when all of the reactions in Table 3 are included. Right panel: solid line represents CH_3COCH_2; dashed line represents CH_3OCH_2, and dotted-dashed line represents CH_3CH_2O.

hot core regions of interstellar clouds, notably towards the galactic center in the cloud Sagittarius (Sgr) B2, and towards the Orion nebula in a variety of positions [56–61]. These sources have rather high gas-phase ($\sim$ 200 K) and grain temperatures ($\sim$ 80 K) compared with non-star-forming dense regions of clouds. However, the recent detection of COMs towards protostellar envelopes at $\sim$ 10 K [21, 62] suggest they might have formed in the cold interstellar medium as well, albeit at lower abundances. Recently, it has been argued that reactive desorption or photodesorption from grain surfaces and radiative association reactions may be possible drivers in the formation of complex molecules in these cold regions [54, 55]. Our results here show that reactions of dimethyl ether, acetone, and ethanol with OH are not sufficiently fast to effect the situation.

Figure 5 shows the percentage gain of the water abundance (solid line) and loss of the OH radical abundance (dashed line) as functions of time when the

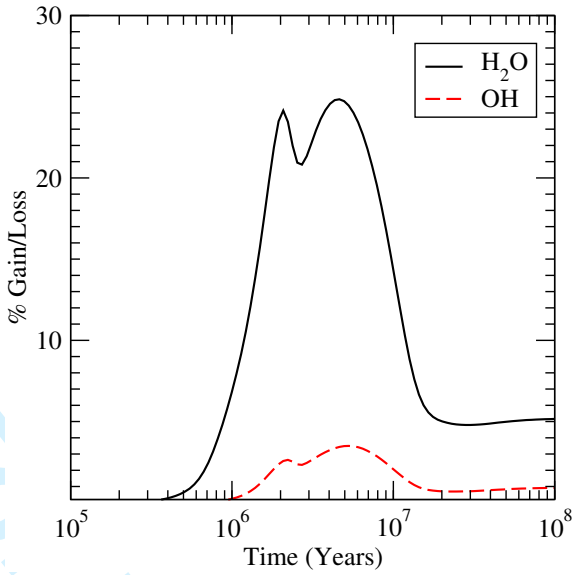

Figure 5. Time evolution of percentage gain of water and percentage loss of OH radical at 10 K when all four OH reactions are included.

temperature is 10 K. For water, the maximum increase is $\approx$ 25% and for OH radical the maximum decrease is $\approx$ 5%, both occurring at $t \approx 5 \times 10^6$ years. At higher temperatures, there is almost no effect caused by the OH reactions. We found the gain and loss to be due mainly to the OH + CH_3OH reaction.

There are other reactions in our astronomical network involving the radicals OH and CN with various neutrals that are known to have activation energy barriers. These reactions, which have not been studied by our methods, have been estimated to have very low rate coefficients at low temperatures. Table 4 lists these reactions, which may have important consequences in astrochemical modelling if they can undergo tunneling efficiently at low temperatures.

Table 4. Additional Reactions With Possible Tunneling Mechanisms

No.	Reaction
1.	$OH + CH_4 \rightarrow CH_3 + H_2O$
2.	$OH + H_2S \rightarrow HS + H_2O$
3.	$OH + H_2O_2 \rightarrow O_2H + H_2O$
4.	$OH + C_2H_2 \rightarrow CCH + H_2O$
5.	$CN + H_2O \rightarrow HCN + OH$
6.	$CN + CH_4 \rightarrow HCN + CH_3$

5. Conclusions

With a new gas-grain network that can be used for assorted interstellar regions in the temperature range 10 - 800 K, we have studied the impact of a number of OH radical-neutral reactions with rate constants that have recently been measured at low temperatures in the laboratory and extrapolated to even lower temperatures.

Of the three temperatures used in our study, the reactions are found to be most important at the lowest temperature, 10 K, which pertains to cold dense interstellar clouds. It was found that for these cold clouds:

- The reaction between OH and CH_3OH is probably the most important of the reactions studied, because it provides an effective and unambiguous gas phase formation route for CH_3O, although it is not a major depletion mechanism for methanol at most times.
- The reactions between OH and acetone, dimethyl ether, and ethanol are not as important because these molecules are of lower abundance than methanol, even in hot cores where their abundances peak. The radicals formed in these reactions are insufficiently abundant to be detected with current observational techniques with the possible exception of the ethoxy radical.
- Finally, all of the OH reactions with neutral species do not play a significant role in the destruction of the OH radical and the formation of water in the gas phase.

Acknowledgements

E. H. gratefully acknowledges the support of the National Science Foundation for his astrochemistry program. He also acknowledges support from the NASA Exobiology and Evolutionary Biology program through a subcontract from Rensselaer Polytechnic Institute. K. A. acknowledges funding from the University of Virginia. R.C. and R.S. gratefully acknowledge the support of the Natural Environment Research Council for the provision of studentships, and M.B. and D.H. acknowledge the National Centre for Atmospheric Science for other funding.

References

[1] E. Herbst and E. F. van Dishoeck, Annu. Rev. Astron. Astrophys., **47**, 427 (2009).
[2] J. Cami, J. Bernard-Salas, E. Peeters and S. E. Malek, Science, **329**, 1180 (2010).
[3] L. J. Allamandola, A. G. G. M. Tielens and J. R. Barker, Astrophys. J. Suppl., **71**, 733 (1989).
[4] V. Wakelam, E. Herbst, J.-C. Loison et al., Astrophys. J. Suppl., **199**, id. 21 (2012).
[5] A. E. Douglas and G. Herzberg, Astrophys. J., **94**, 381 (1941).
[6] W. S. Adams, Astrophys. J., **93**, 11 (1941).
[7] A. McKellar, Publ. Astron. Soc. Pac. **52**, 187 (1940).
[8] W. Iqbal, K. Acharyya and E. Herbst, Astrophys. J., **784**, id. 139 (2014).
[9] L. Spitzer, Jr., *Physical Processes in the Interstellar Medium* (John Wiley & Sons, New York, 1998).
[10] W. D. Geppert and M. Larsson, Chem. Rev., **113**, 8872 (2013).
[11] E. Herbst and W. Klemperer, Astrophys. J., **185**. 505 (1973).
[12] J. B. Marquette, B. R. Rowe, G. Dupeyrat and E. Roueff, Astron. Astrophys., **147**, 115 (1985).
[13] D. Chastaing, P. L. James, I. R. Sims, I. W. M. Smith, Phys. Chem. Chem. Phys., **1**, 2247 (1999).
[14] A. Canosa, F. Goulay, I. R. Sims, B. R. Rowe, in *Low Temperature and Cold Molecules*, ed. by I. W. M. Smith (Imperial Collage Press, London), 55-120 (2008).
[15] I. W. M. Smith, A. M. Sage, N. M. Donahue, E. Herbst and D. Quan, Faraday Discussions, **133**, 137 (2006).
[16] D. L. Baulch, C. T. Bowman, C. J. Cobos, R. A. Cox, T. Just et al., J. Phys. Chem. Ref. Data, 34, 757 (2005).
[17] R. J. Shannon, M. A. Blitz, A. Goddard and D. E. Heard, Nat. Chem., **5**, 745 (2013).
[18] R. J. Shannon, R. L. Caravan, M. A. Blitz and D. E. Heard, PCCP, 14, 3466, (2014).
[19] R. L. Caravan, R. J. Shannon, T. Lewis, M. A. Blitz and D. E. Heard, J. Phys. Chem. A, DOI: 10.1021/jp505790m (2014).
[20] J. C. Gomez-Martin, R. L. Caravan, M. A. Blitz, D. E. Heard and J. M. C. Plane, J. Phys Chem. A, **118**, 2693 (2014).
[21] J. Cernicharo, N. Marcelino, E. Roueff, M. Gerin, A. Jimenez-Escobar and G. M. Munoz Caro, Astrophys. J., **759**, id. L43 (2012).
[22] R. T. Garrod, S. L. W. Weaver and Herbst, E., Astrophys. J., **682**, 283 (2008).
[23] N. Harada, E. Herbst and V. Wakelam, Astrophys. J., **721**, 1570 (2010).
[24] T. I. Hasegawa, E. Herbst and C. M. Leung, Astrophys. J. Suppl., **82**, 167 (1992).
[25] Q. Chang and E. Herbst, Astrophys. J., **787** , id. 135 (2014).
[26] S. Cazaux and A. G. G. M. Tielens, Astrophy. J., **604**, 222 (2004).

[27] W. Iqbal, K. Acharyya and E. Herbst, Astrophys. J., **751**, id. 58 (2012).
[28] V. G. Anicich, J. Phys. Chem. Ref. Data, **22**, 1469 (1993).
[29] D. E. Woon and E. Herbst, Astrophys. J, **185**, 273 (2009).
[30] D. Gerlich and S. Horning, Chem. Rev., **92**, 1509 (1992).
[31] E. Herbst, Nature, **289**, 656 (1981).
[32] P. B. Rimmer, E. Herbst, O. Morata and E. Roueff, Astron. Astrophys., **537**, id. A7 (2012).
[33] R. Gredel, S. Lepp, A. Dalgarno and E. Herbst, Astrophys. J., **347**, 289 (1989).
[34] V. Wakelam, I. W. M. Smith, E. Herbst, J. Troe et al., Space Science Reviews, **156**, 13 (2010).
[35] E. Herbst & T. J. Millar, in *Low Temperatures and Cold Molecules* edited I. W. M. Smith (London, Imperial College Press, 2008), pp 1-54.
[36] V. Pirronello, O. Biham, C. Liu, L. Shena and G. Vidali, Astrophys. J., **483**, L131 (1997).
[37] V. Pirronello, C. Liu, L. Shena and G. Vidali, Astrophys. J., **475**, L69 (1997).
[38] V. Pirronello, C. Liu, J. E. Riser and G. Vidali, Astron. Astrophys., **344**, 681 (1999).
[39] M. Minissale, E. Congiu and F. Dulieu, J. Chem. Phys., **140**, id. 074705 (2014).
[40] M. Ruaud, J. C. Loison, K. M. Hickman, P. Gratier, F. Hersant and V. Wakelam, Mon. Not. R. Astron. Soc., **447**, 4004 (2015).
[41] R. T. Garrod, V. Wakelam, & E. Herbst, Astron. Astrophys., **467**, 1103 (2007)
[42] F. Dulieu, E. Congiu, J. Noble, S. Baouche, H. Chaabouni, A. Moudens, M. Minissale and S. Cazaux, Nature Sci. Rep., **3**, id. 1338 (2013).
[43] D. P. Ruffle and E. Herbst, Mon Not. R. Astron. Soc., **319**, 837 (2000).
[44] G. A. Cruz-Diaz, G. M. Munoz-Caro, Y.-J. Chen and T.-S. Yih, Astron. Astrophys., **562**, id A119 (2014).
[45] G. A. Cruz-Diaz, G. M. Munoz-Caro, Y.-J. Chen and T.-S. Yih, Astron. Astrophys., **562**, id A120 (2014).
[46] G. A. Cruz-Diaz, G. M. Caro, G. M. Munoz and Y.-J. Chen, Mon. Not. R. Astron. Soc., **439**, 2370 (2014).
[47] K. I. Öberg, et al. Astrophys. J., **678**, 1032 (2008).
[48] K. I. Öberg, E. F. van Dishoeck and H. Linnartz, Astron. Astrophys., **496**, 281 (2009).
[49] K. I. Öberg, H. Linnartz, R. Visser and E. F. van Dishoeck, Astrophys. J., **693**, 1209 (2009).
[50] G. M. Munoz Caro, A. Jimenez-Escobar, J. A. Martin-Gago, C. Rogero, C. Atienza, S. Puertas, J. M. Sobrado and J. Torres-Redondo, Astron. Astrophys., **522**, id. A108 (2010).
[51] M. Bertin, E. C. Fayolle, C. Romanzin, H. A. M. Poderoso, X. Michaut, L. Philippe, P. Jeseck, K. I. Öberg, H. Linnartz and J.-H. Fillion, Astrophys. J., **779**, id. 120 (2013).
[52] T. Hasegawa, & E. Herbst, Mon Not. R. Astron. Soc., **261**, 83 (1993).
[53] I. W. M. Smith, E. Herbst and Q. Chang, Mon Not. R. Astron. Soc., **350**, 323 (2004).
[54] N. Balucani, C. Ceccarelli and V. Taquet, Mon Not. R. Astron. Soc., submitted for publication.
[55] A. I. Vasyunin and Eric Herbst, Astrophys. J., **769**, 34 (2013).
[56] F. Combes, M. Gerin, A. Wootten, G. Wlodarczak, F. Clausset and P. J. Encrenaz, Astron. Astrophys., **180**, L13 (1987).
[57] T.-C. Peng, D. Despois, N. Brouillet, A. Baudry, C. Favre, A. Remijan, A. Wootten, T.L.Wilson, F. Combes, and G. Wlodarczak, Astron. Astrophys., **554**, id. A78 (2013).
[58] L. E. Snyder, F. J. Lovas, D. M. Mehringer, N. Y. Miao, Y.-J. Kuan, J. M. Hollis and P. R. Jewell, Astrophys. J., **578**, 245 (2002).
[59] N. Brouillet, D. Despois, A. Baudry, T.-C.Peng, C. Favre, A. Wootten, A.J. Remijan, T. L. Wilson, F. Combes and G. Wlodarczak, Astron. Astrophys., **550**, id. A46 (2013).
[60] B. Zuckerman, B. E. Turner, D. R. Johnson, F. J. Lovas, N. Fourikis, P. Palmer, M. Morris, A. E. Lilley, J. A. Ball and F. O. Clark, Astrophys. J., **196**, 99 (1975).
[61] T. J. Millar, P. D. Brown, H. Olofsson and A. Hjalmarson, Astron. Astrophys., **205**, 5 (1988).
[62] A. Bacmann, V.Taquet, A. Faure, C. Kahane and C. Ceccarelli, Astron. Astrophys., **541**, L12 (2012).